Life Sciences in Space Research 15 (2017) 1–10

Contents lists available at ScienceDirect

Life Sciences in Space Research

journal homepage: www.elsevier.com/locate/lssr

Payload hardware and experimental protocol development to enable future testing of the effect of space microgravity on the resistance to gentamicin of uropathogenic *Escherichia coli* and its σ^s-deficient mutant

A.C. Matin[a,*], J.-H. Wang[a], Mimi Keyhan[a], Rachna Singh[a], Michael Benoit[a], Macarena P. Parra[b,*], Michael R. Padgen[b], Antonio J. Ricco[b,*], Matthew Chin[b], Charlie R. Friedericks[b], Tori N. Chinn[b], Aaron Cohen[b], Michael B. Henschke[b], Timothy V. Snyder[b], Matthew P. Lera[b], Shannon S. Ross[b], Christina M. Mayberry[b], Sungshin Choi[b], Diana T. Wu[b], Ming X. Tan[b], Travis D. Boone[b], Christopher C. Beasley[b], Matthew E. Piccini[b], Stevan M. Spremo[b]

[a] *Department of Microbiology & Immunology, Stanford School of Medicine, Stanford, CA 94305, USA*
[b] *NASA Ames Research Center, Moffett Field, CA 94035, USA*

ARTICLE INFO

Keywords:
Bacterial antibiotic resistance
Microgravity
Low-shear modeled microgravity (LSMMG)
Stress response
Sigma S
Stationary phase
Uropathogenic *E. coli* (UPEC)
EcAMSat
Nanosatellite
Cubesat
Gentamicin
Alamar blue
Sigma-s deletion

ABSTRACT

Human immune response is compromised and bacteria can become more antibiotic resistant in space microgravity (MG). We report that under low-shear modeled microgravity (LSMMG), stationary-phase uropathogenic *Escherichia coli* (UPEC) become more resistant to gentamicin (Gm), and that this increase is dependent on the presence of σ^s (a transcription regulator encoded by the *rpoS* gene). UPEC causes urinary tract infections (UTIs), reported to afflict astronauts; Gm is a standard treatment, so these findings could impact astronaut health. Because LSMMG findings can differ from MG, we report preparations to examine UPEC's Gm sensitivity during spaceflight using the *E. coli Anti-Microbial Satellite* (*EcAMSat*) as a free-flying "nanosatellite" in low Earth orbit. Within *EcAMSat's* payload, a 48-microwell fluidic card contains and supports study of bacterial cultures at constant temperature; optical absorbance changes in cell suspensions are made at three wavelengths for each microwell and a fluid-delivery system provides growth medium and predefined Gm concentrations. Performance characterization is reported here for spaceflight prototypes of this payload system. Using conventional microtiter plates, we show that Alamar Blue (AB) absorbance changes can assess the Gm effect on *E. coli* viability, permitting telemetric transfer of the spaceflight data to Earth. Laboratory results using payload prototypes are consistent with wellplate and flask findings of differential sensitivity of UPEC and its Δ*rpoS* strain to Gm. if σ^s plays the same role in space MG as in LSMMG and Earth gravity, countermeasures discovered in recent Earth studies (aimed at weakening the UPEC antioxidant defense) to control UPEC infections would prove useful also in space flights. Further, *EcAMSat* results should clarify inconsistencies from previous space experiments on bacterial antibiotic sensitivity and other issues.

1. Introduction

This paper is concerned with the development of a system of hardware and experimental protocols, to be deployed aboard a free-flying "nanosatellite", for determining the effect of space microgravity (MG) on the resistance of uropathogenic *Escherichia coli* [UPEC; strain AMG1 (Wang et al., 2014)] to the antibiotic gentamicin (Gm). This system is termed the *E. coli* Antimicrobial Satellite (*EcAMSat*) payload platform.

UPEC is a causative agent of urinary tract infection (UTI), which has been reported in astronauts (Singh and Matin, 2016), and Gm is standard treatment for this disease. In our previous studies using conventional Earth experimental systems, we have shown that proteins controlled by the sigma factor, σ^s (product of the *rpoS* gene), contribute to the Gm resistance of UPEC; these proteins belong to the antioxidant defense of this bacterium and we have identified several of them. This opens the way for enhancing the effectiveness of Gm against UPEC by devising means (e.g., small-molecule inhibitors) to impair the activity of these proteins (Wang et al., 2014). (σ^s is the master regulator of the general stress response (GSR) in UPEC and several other bacteria; GSR

* Corresponding authors.
E-mail addresses: a.matin@stanford.edu (A.C. Matin), macarena.p.parra@nasa.gov (M.P. Parra), antonio.j.ricco@nasa.gov (A.J. Ricco).

http://dx.doi.org/10.1016/j.lssr.2017.05.001
Received 24 February 2017; Accepted 7 May 2017

is activated under stressful conditions and confers broad resistance on bacteria to diverse antimicrobial agents (Hengge-Aronis, 2002b; Matin, 1991, 2014; Matin et al., 1989)).

We show here (*Results*) that UPEC cultivation in low-shear modeled microgravity (LSMMG) makes it more resistant to Gm compared to its normal gravity-cultivated counterpart and that this enhanced resistance is also dependent on σ^s. This is consistent with previous findings from our and other groups showing that LSMMG cultivation makes UPEC and other bacteria resistant to disinfectant agents, e.g., low pH, high osmolarity, and ethanol (Gao et al., 2001; Lynch et al., 2004). We also showed that the LSMMG-conferred resistance to the disinfectants depends on σ^s (Lynch et al., 2004). Given that the latter regulates the stress-induced GSR mentioned above, the σ^s-dependence of the LSMMG effect suggests that UPEC responds to this condition as a stress.

We are interested in determining whether the UPEC Gm resistance increases also in space MG in a σ^s-dependent manner. While LSMMG may approximate space MG, its findings are not necessarily applicable to the latter. For example, the virulence of *Listeria monocytogenes*, methicillin-resistant *Staphylococcus aureus* (MRSA), and *Enterococcus faecalis* were affected differently by spaceflight compared to LSMMG (Hammond et al., 2013); in *Salmonella enterica* serovar Typhimurium, the virulence genes *sipD* and *sipC* were differently regulated under the two conditions (Wilson et al., 2002).

The *EcAMSat* nanosatellite, scheduled to be launched in 2017, will be used to address the above and related questions. Should the Gm resistance of UPEC increase also in space MG, it would constitute a clear hazard to astronaut health, especially given that human immune response is weakened in space MG (Bascove et al., 2009; Crucian et al., 2009; Mehta et al., 2000; Yi et al., 2016). Further, should it also turn out that the increase in GM resistance in space MG is dependent on σ^s, measures discovered in Earth studies mentioned above, namely impairing the antioxidant proteins (Wang et al., 2014), would be likely to prove useful for increasing Gm effectiveness in treating UPEC infections in space flight. Moreover, indication would be forthcoming that UPEC responds to space MG as a stress.

As in our previous work (Wang et al., 2014; Matin, 2009; Zgurskaya et al., 1997), our focus here is on stationary-phase UPEC. This is because: (a) due, for example, to lack of nutrients or the presence of oxidative stress, this late-growth phase is often experienced by bacteria in the human host (Matin, 2014; Hengge-Aronis, 2002a, Kolter et al., 1993); (b) it is in the stationary phase that bacteria express many of the virulence traits required for disease causation (Sonenshein, 2005; Llorens et al., 2010; Cabeen, 2014; Dalebroux et al., 2010; Mangan et al., 2006; Mouslim and Hughes, 2014; Roop et al., 2003) (an example is UPEC Type I fimbriae, which it uses in bladder colonization (Kau et al., 2005a, b)); and (c) bacteria in this phase are hard to eradicate, because the GSR activated in this phase makes bacteria broadly resistant (Matin, 1991, 2014).

Nanosatellite systems, such as *GeneSat, PharmaSat*, and *O/OREOS*, were developed by NASA to augment the capability for studying microbial behavior in space MG over that offered by the Space Shuttle and the International Space Station (Nicholson et al., 2011; Woellert et al., 2011; Ricco et al., 2011). The nanosatellite platforms do not require crew member participation and have the advantage of permitting experimentation in multiple orbital locations (Nicholson et al., 2011; Woellert et al., 2011; Ricco et al., 2011). The *PharmaSat* platform has previously been used to determine the effect of flight in a low Earth orbit (under conditions that provided $<10^{-3} \times$ Earth gravity) on the sensitivity of the yeast *Saccharomyces cerevisiae* to the antifungal agent voriconazole (Ricco et al., 2011). In developing the *EcAMSat* payload, we built upon the *PharmaSat* system to make it suitable for work with bacteria, and have optimized it for spaceflight implementation of the experiments reported here. We have tested the *EcAMSat* payload system using the same experimental command sequence that will be employed during space flight and show here that it faithfully reproduces the previously reported difference in sensitivity to Gm between UPEC strain AMG1 and its isogenic *rpoS* mutant (Wang et al., 2014).

2. Materials and methods

2.1. LSMMG effect on Gm sensitivity

To determine the effect of cultivation under LSMMG on UPEC, strain AMG1, and its isogenic Δ*rpoS* mutant (Wang et al., 2014), the two strains were cultivated in high-aspect-ratio-vessel (HARV) reactors as described previously (Lynch et al., 2004). Pairs of the reactors were rotated about appropriate axes: vertical for normal gravity ('HARV NG') and horizontal for LSMMG conditions. 50 mL of Luria broth (LB) medium was used in each vessel. Overnight conventional-flask LB cultures were used as inoculum; the starting absorbance at 660 nm (A_{660}) was 0.1, and the HARVs were rotated at 25 rpm. Following 24-h incubation (37 °C), the stationary-phase cells were harvested from the HARVs, re-suspended in M9 salts (referred to from hereon as 'M9') to an A_{660} of 0.4, and mixed with sufficient Gm to give a final concentration of 16 μg/mL. Gm at 16 μg/mL represents the minimum inhibitory concentration (MIC) for resistant (*R*) Gram-negative bacteria. (Gm MICs for intermediate (*I*) and sensitive (*S*) strains are 8 and 4 μg/mL, respectively.)

After 24-h incubation (37 °C) under static conditions, viability was determined by counting colony-forming units (CFU) using LB plates.

2.2. Determination of the suitability of Alamar Blue to assess Gm effect on UPEC viability

To test the effect of space MG in spaceflight experiments, a method for UPEC viability assessment is needed, the results of which can be transmitted from space to Earth via telemetry. The dye Alamar Blue (AB) was used for this purpose in the *PharmaSat* experiment, as it changes color upon reduction (Parra et al., 2009). AB can be reduced by several cellular electron donors (e.g., NAD(P)H, FADH and several cytochromes) and thus its reduction can reflect cell viability. The *PharmaSat* mission involved exponentially growing cells, and it is in this phase that AB is recommended for assessing cell viability (Rampersad, 2012). Our work, however, involved stationary-phase cells and since AB-based measurements can also be affected by factors such as the nature of mutations and test compound or drugs (Rampersad, 2012), it was necessary to determine whether, under the conditions used, AB reduction kinetics could accurately reflect changes in viability of the stationary-phase cells of the two strains by Gm treatment.

Reduction of AB is indicated by a change in its color from dark blue, as measured by red absorbance at 615 nm (A_{615}) to magenta, as measured by green absorbance at 525 nm (A_{525} nm), resulting in concomitant decrease and increase of the absorbance, respectively, at the two wavelengths. Both the reduced and oxidized AB have weak absorbance at 470 nm, and measurement at this wavelength reflects medium turbidity and can thus be used to monitor changes in cell population.

Measured absorbance at 615, 525, and 470 nm only approximate the respective amounts of oxidized AB, reduced AB, and cell-related turbidity. To more accurately determine these parameters, we measured complete visible absorbance spectra of oxidized AB, reduced AB, and a suspension of *E. coli*. We then used the absorbance values at the three measurement wavelengths to calculate "cross terms" that correct for the fact that the absorbance spectrum of (blue) oxidized AB has a shoulder at 525 nm and a tail at 470 nm, that the spectrum of (magenta) reduced AB also has a tail at 470 nm, and that light scattering by the bacteria occurs throughout the visible range, varying with a weak linear wavelength dependence. All graphics and results reported below for quantities of oxidized AB, reduced AB, and cell turbidity have been corrected accordingly.

To determine if the AB-conversion method can be used for assessing

UPEC viability, the wild type and the Δ*rpoS* strains were grown in conventional laboratory flasks shaken overnight at 200 rpm in 1/6-strength LB at 37 °C. As before (Zgurskaya et al., 1997), growth under these conditions was complete within 6 h, allowing some 8 h in stationary phase, permitting activation of GSR in the wild type, but not in the mutant missing the *rpoS* gene, which, as stated, is required for the activation of GSR (Matin, 2014). The cultures were then diluted to an A_{600} of 0.45 in M9. Gm (Sigma-Aldrich, St. Louis, MO) was added to both the wild type and the mutant cultures to a final concentration of 16 μg/mL; a parallel aliquot of cell suspension of each strain without the drug served as control. Following 24-h incubation without shaking, 1.8 mL of the cultures were transferred to test tubes to which 200 μL of 10x AB (ThermoFisher Scientific, Grand Island, NY) were added. To monitor changes in AB absorption, the cultures were dispensed in microtiter plate wells (Thermo Scientific, Waltham, MA), each well receiving 0.25 mL. Appropriate control solutions in other rows of the plates were also in 0.25 mL quantities, and five wells were used for each condition. Absorption changes at 470, 525, and 615 nm were measured in a microplate reader (Biochrom US, Holliston, MA); data were acquired by DigiRead software (ASYS Hitech, Holliston, MA) and transferred to Excel (Microsoft, Redmond, WA) for analysis.

2.3. EcAMSat payload system

The *E. coli* in this setup are placed in the payload hardware in a 48-well fluidic card (Fig. 1; Micronics, Redmond, WA). The cards are made from laser-cut layers of poly(methylmethacrylate), bonded together with pressure-sensitive acrylic adhesive (9471LE on 51-μm-thick Melinex 455 polyester carrier, 3 M; St. Paul, MN). Each well (4.0 mm diameter x 7.8 mm long; 100 μL volume) is fitted at its inlet and outlet with 0.2-μm filters (nylon fiber; Sterlitech, Kent, WA) to prevent cell leakage. Well tops and bottoms are sealed by 50-μm-thick air-and-CO_2-permeable optical-quality poly(styrene) membranes. Attached to both sides of the card are thermal spreaders (thin aluminum plates), each containing three embedded AD590 temperature sensors that provide output current directly proportional to absolute temperature (Analog Devices, Norwood, MA); a thin-film heater fabricated from kapton tape and patterned metal conductors (Minco, Minneapolis, MN) is affixed to the opposite side of each spreader plate, relative to the fluidic card, and controlled in closed-loop fashion using the temperature-sensor outputs. Each well is equipped with its own 3-color LED (LTST-C17FB1WT; Lite-On Technology Corp., Taiwan); a photodetector (Model no. TSL237T; AMS-TAOS USA, Plano, TX) at the opposite end of each well converts the transmitted light intensity to a proportional frequency, from which absorbance values can be calculated. (No moving parts are associated with the optical measurements.) The card, thermal spreaders, and printed-circuit (PC) boards supporting the LEDs and photodetectors, which are placed on opposite sides of the fluidic card, constitute the "card stack" (see the cross section, upper right in Fig. 1).

The card fluid-delivery system (Fig. 1) includes eleven electrically-actuated solenoid valves (SVs, LHDA0531315HA; The Lee Co., Westbrook, CT); a diaphragm pump for high-flow-rate fluid mixing, circulation, and priming of tubing (NF 5S; KNF Neuberger, Trenton, NJ); a precision metering pump (LPVX0502600BC; The Lee Co.) to prepare

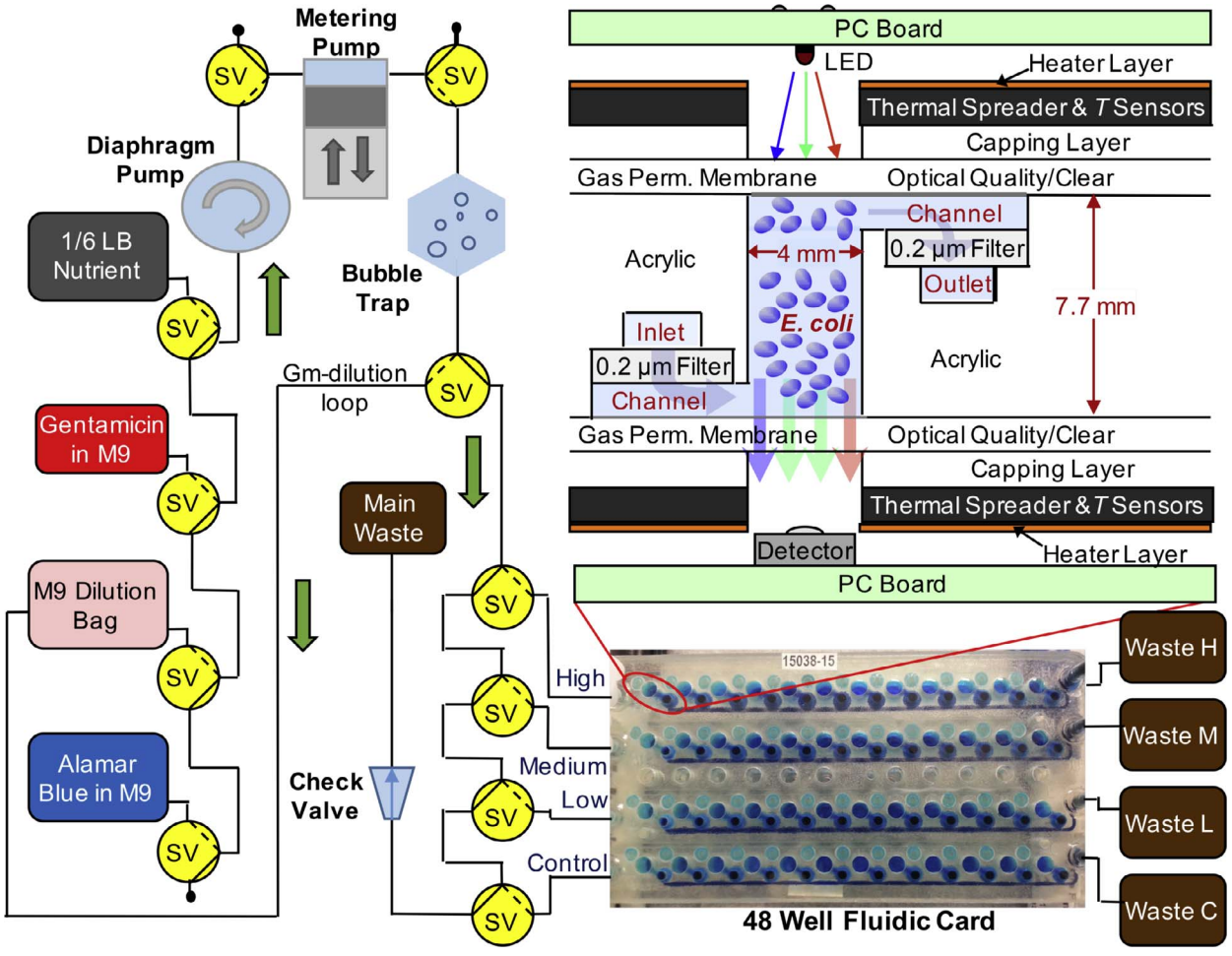

Fig. 1. Schematic diagram of EcAMSat fluidic system (at left) connected to EcAMSat 48-well fluidic card (at lower right). A single fluidic well is also shown in cross section (top right). SV = 3-way solenoid valve; arrows show direction of fluid flow; Waste H, M, L, C collect the flow-through from the High, Medium, Low, and Control banks of 12 wells each; other components are as marked.

and deliver the desired concentrations and volumes of antibiotic and other reagents; three 35-mL and six 25-mL reagent bags (fluorinated ethylene propylene, FEP; American Fluoroseal/Saint-Gobain, Gaithersburg, MD); a bubble trap (custom fabricated by NASA Ames); and a check valve (Smart Products; Morgan Hill, CA) to prevent waste fluids from flowing back into the system. The 48 wells are configured in 4 fluidically independent rows or "banks" of 12 each (labeled "High", "Medium", "Low", and "Control" in Fig. 1, indicating the relative Gm concentrations that were administered). Each bank on the inlet side of the card is connected to the normally-closed port of one SV and, on the outlet side, to a 25-mL waste bag partially filled with M9; pressurization (~7 kPa) of these waste bags by means of a spring-loaded metal plate replaces any fluid that evaporates over time from the wells through their permeable membrane cover. The nutrient (1/6-strength LB), antibiotic (Gm), antibiotic dilution medium (M9), and AB bags are also attached to SV normally-closed ports (Fig. 1). A Gm-dilution loop is created by attaching the M9 bag via another SV near the outlet of the bubble trap, which is placed ahead of the point of fluid delivery to the card. The main waste bag collects the previous contents of the tubing each time it is filled with a new reagent (see below) prior to delivery to the card.

Fig. 2A and B show, respectively, the assembled *EcAMSat* payload fluidic system hardware and the hermetically sealed containment vessel (internal volume ~1.2 L) in which the system is housed. The sealed payload containment vessel is integrated with the spacecraft "bus", which includes the power, communications, data-handling, and control functions. The completed nanosatellite has overall dimensions of 10 × 22 × 36 cm.

2.4. AB-mediated assessment of Gm effect in the EcAMSat payload

The wild type and Δ*rpoS* mutant of UPEC were grown as described above, rinsed with M9 (3x), and diluted in M9 to an A_{600} of 1.0. In a sterile biosafety cabinet, 5 µL aliquots of each strain were loaded in alternating wells of the 48-well fluidic card so that six of the 12 wells per bank contained the wild type and six wells, the mutant. The card was sealed and purged with CO_2 to facilitate bubble-free filling of the channels and wells: any CO_2 bubbles remaining after priming with degassed M9 dissolved readily as additional M9 flowed through the wells. The card was manually primed with a syringe containing degassed M9 connected to the outlet. A second empty syringe at the inlet with its plunger drawn back served to generate a slight vacuum (which assists bubble-free filling of wells). After filling and until connection was made to the fluidic system, the card remained under pressure (~4.4 kPa), arising from a bag containing M9 hanging approximately 45 cm above the card. This served to replace any fluid lost by evaporation through the permeable membranes, thereby preventing bubble formation in the wells. The rest of the sterile fluidic system was filled with the appropriate solutions (see Fig. 1), assembled with the rest of the payload hardware, and then sealed in the hermetic containment vessel; as explained above, slightly pressurized M9 in the waste bags continued to compensate for any evaporation. As placement in the containment vessel eliminated further need for a sterile environment, the assembled payload system was removed from the biosafety cabinet and attached to a benchtop "rotisserie" apparatus; this rotated the payload successively clockwise and counterclockwise by nearly one full rotation with a period of ~80 s, preventing cell settling. The experiments were run using ground-support equipment, i.e., a desktop computer and power supply, and employed a "space-flight-like" command sequence.

In experiments involving the microtiter plates (see above), cells were incubated without shaking only when being treated with the drug and in the absence of nutrients. A biofilm formation by the cells under these conditions does not occur and none was found. Given the different setup of the *EcAMSat* payload, whether a biofilm could form in this platform and its potential effects on the interpretation of the results are considered in subsequent sections.

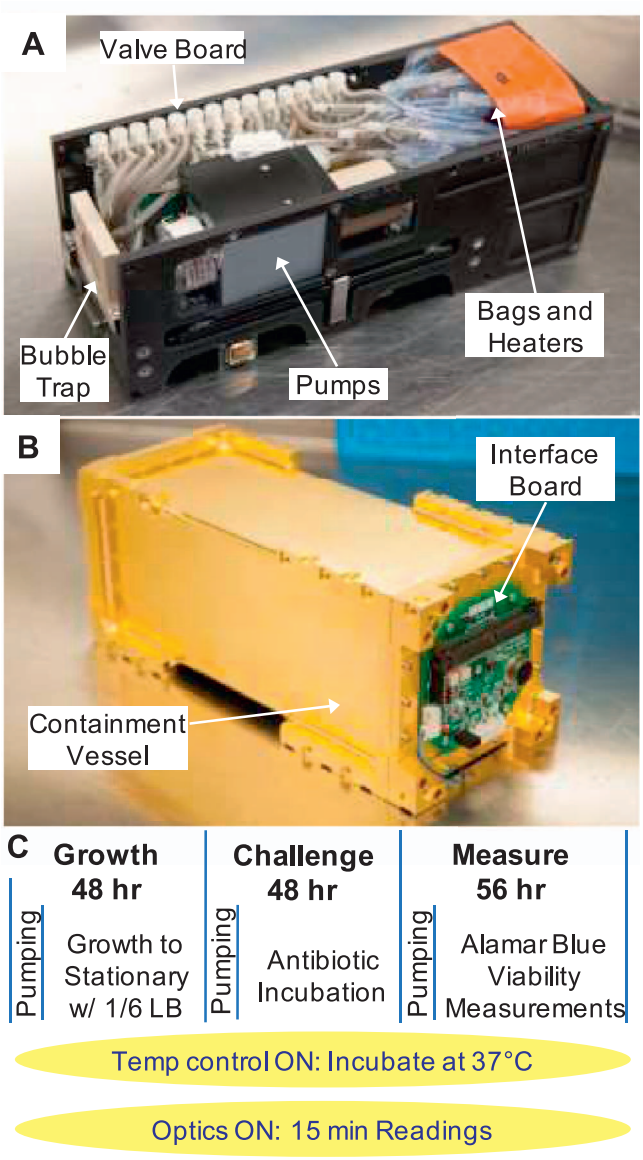

Fig. 2. **(A)** Fully assembled EcAMSat biological/fluidic/optical/thermal payload system; **(B)** its hermetic payload containment vessel with electrical interface board; overall size ~10 × 10 × 20 cm. **(C)** Chronological summary of the sequence of operations and measurements for the ground experiments conducted to date; the spaceflight system will follow the same timeline.

To start the viability measurements, the 3-color LEDs with emissions at the above-mentioned wavelengths were sequentially energized, one color and one well at a time. The photodetector of each well converted the transmitted light intensity of the individual colors to proportional frequencies, permitting calculation of absorbance. (During the space-flight experiments, the stored frequencies will be telemetrically transferred to Earth from the satellite.) The measurements for each well were taken every 15 min. The payload system was warmed to 37 °C for ~3 h by the heaters and thermal spreaders with closed-loop temperature control using the mean value from the six temperature sensors. 1/6-strength LB was pumped into each bank in turn, starting with the control bank, replacing the M9. The pumping phase lasted for 2 h per bank (see *Results* section for total durations of the various phases). The cells were allowed to grow to stationary phase, in which the GSR is activated. Next, the metering pump delivered M9 to the control bank, each well receiving ~4x its 100 µL volume to reach at least 90% exchange. The metering pump then extracted a small, measured

amount of concentrated Gm from the antibiotic bag and delivered it to the M9 dilution bag (Fig. 1); the Gm-dilution loop was opened and the diaphragm pump operated to mix the antibiotic and M9. After delivery of the resultant lowest concentration of Gm to the Low bank (~4x exchange), the process was repeated to prepare and then deliver the medium and high Gm concentrations to the Medium and High banks, respectively. Following incubation with Gm, AB was added, displacing the M9 in the Control bank and the Gm in the other banks.

2.5. Determination of 'stasis' effect

An approximately six-week delay is expected between loading of cells and reagents into the satellite payload hardware and initiation of the experiments in space. To determine the effect of such stasis on cell viability, Gm strength, and AB properties, the cells were incubated without shaking in M9 for 10 weeks and the reagents were stored for this duration in the same types of bags that will be used for the space mission. Cell viability was determined by CFU count; the Gm and AB activities were assessed by comparing the effect of aged reagents with fresh ones in cell killing and assessing cell activity, respectively.

3. Results

3.1. LSMMG cultivation makes UPEC more resistant to Gm but not its Δ*rpoS* mutant

We examined the effect of LSMMG cultivation on Gm sensitivity of UPEC: cells were cultivated in HARV reactors to stationary phase and then exposed to Gm for 24 h. LSMMG-grown UPEC was significantly more resistant to Gm than the control culture grown under HARV NG conditions (29 ± 2% vs. 18.6 ± 1.2% survival, $p < 0.01$). This is reminiscent of the well-established effect of LSMMG on enhanced resistance of *E. coli* to disinfectant agents, as mentioned in the Introduction (Gao et al., 2001; Lynch et al., 2004). Consistent with the results of cells grown under NG in conventional flasks (Wang et al., 2014), the Δ*rpoS* mutant was more sensitive to the drug than the wild type also under the HARV NG conditions (2.33 ± 0.09% vs. 18.6 ± 1.2% survival, $p < 0.01$). Furthermore, as in the case of disinfectant agents, the mutant, unlike the wild type, failed to show increased Gm resistance under LSMMG; indeed, under these conditions, it was more sensitive than its HARV NG-grown counterpart (0.21 ± 0.07% vs 2.33 ± 0.09% survival, $p < 0.001$).

Thus, LSMMG stress makes *E. coli* broadly resistant, including to an important drug, and this effect is σ^s-dependent. As stated in the Introduction, LSMMG may not fully represent space MG conditions, and thus these results and their medical implications for space travelers cannot be taken as necessarily relevant to space MG, unless demonstrated directly under the latter conditions. *EcAMSat* payload platform was therefore tested for suitability for this purpose.

3.2. Alamar Blue absorption changes permit determination of UPEC viability

For reasons mentioned in Materials and Methods, we tested the suitability of AB as reporter for assessing stationary phase UPEC viability; this included determining whether AB-assessed viability would show the increased sensitivity to Gm of the Δ*rpoS* strain. The wild type and the Δ*rpoS* mutant were grown in LB to stationary phase; 12 h were allowed in this phase to activate the GSR. They were treated with 16 μg/mL Gm for 24 h, and viability was determined by monitoring AB reduction for 6 h (Fig. 3), using a well-plate reader. See legend to Fig. 3 for details and statistics.

In summary, the results show that the amount of AB reduced by both strains when treated with Gm is less than for the respective untreated controls, but that Gm treatment diminishes the dye reduction capability of the mutant to a higher extent than that of the wild type (Fig. 3E). Fig. 3F compares the relative magnitude of the effect of the antibiotic on the wild type and the mutant using the 6-h endpoint data of Fig. 3E. The bars represent percent AB reduced in the presence of Gm divided by that reduced in its absence for each strain and show that while the dye reduction by the Gm-treated wild type was 74% compared to that of its untreated counterpart cells, this value was diminished to 60.5 ± 3.2% for the mutant, i.e., some 14% less. Thus, in both strains changes in AB absorbance reflecting viability agree qualitatively with the Gm effect on the two strains found by CFU measurements (Wang et al., 2014) (Fig. 3A). While qualitative, it is clear that AB measurements nevertheless are an accurate index of cell viability.

3.3. The EcAMSat system permits efficient dilution and exchange

It is of course essential that the dilutions and exchanges needed to conduct the experiments in the *EcAMSat* hardware be accurately accomplished. Antibiotic is carried in the payload in a concentrated form (400 μg/mL) and will require dilution to the planned three specific concentrations during the space experiment. To determine the accuracy of the dilution process, a 1% solution of yellow dye (trisodium 5-hydroxy-1-(4-sulfonatophenyl)-4-[(*E*)-(4-sulfonatophenyl)diazenyl]-1*H*-pyrazole-3-carboxylate, commonly called tartrazine; absorbance: 414 nm) in M9 was loaded into the antibiotic bag in place of Gm (see Figs. 1 and 2). The payload was assembled but not loaded into the hermetic containment vessel so that the system was in near-flight-like configuration but with the tubing accessible during the pumping. A_{414} of the dye samples diluted using the *EcAMSat* payload system, was measured, and the equivalent Gm dose was calculated using a standard curve. This was done for three different "builds" of the fluidic system (relating to the use of different fluidic cards, sets of tubing, pumps, and valves). Fig. 4A shows measured dilutions using dye concentrations that correspond to Gm doses of 3.5, 14.6, and 52 μg/mL; they correspond to a systematic error of 9–16% below the intended concentrations. The coefficients of variance are 4–5% for the medium at high concentrations and 20% for the low; the latter was unsurprising due to its high dilution ratio. Because of the low degree of the deviations from the specified concentrations, and the fact that they will occur in both the spaceflight and ground control systems, which will be run in parallel, they are not expected to significantly impact the results.

Fluid exchange in the banks is required to make transitions from initial stasis buffer to the following phases: feeding-and-starvation; Gm dosing; and AB-mediated viability measurement. To quantify the accuracy of these exchanges, 0.2% blue food dye in M9 was loaded in the AB bag and pumped into all four banks of the card using the same flow rate and duration as for the planned exchanges in the actual experiments (4x volume exchange – over 2 h per bank).

The payload was then disassembled, and the absorbance of the dye in the wells of the banks at A_{620} was measured in a plate reader. To ascertain the extent to which the replacement of M9 by the dye was short of 100%, absorbance of the wells was first determined when the wells were saturated with the dye; this was accomplished by hanging the dye-filled bag ~45 cm above the card, and allowing 6 mL of the dye to flow through each bank (the volume of an entire bank of 12 wells is ~1.5 mL, so this corresponds to a 4x exchange). Background absorbance was determined with M9 ($A_{620} = 0$) alone in the wells. The dye absorbance was then determined following pumping under the actual experimental conditions. Background absorbance was subtracted from both measurements, and dye absorbance under the experimental conditions was calculated as percent of absorbance at 100% exchange. Fig. 4B shows that with some bank-to-bank and test-to-test variability, the exchange efficiency in the wells was near, and often greater, than 90%.

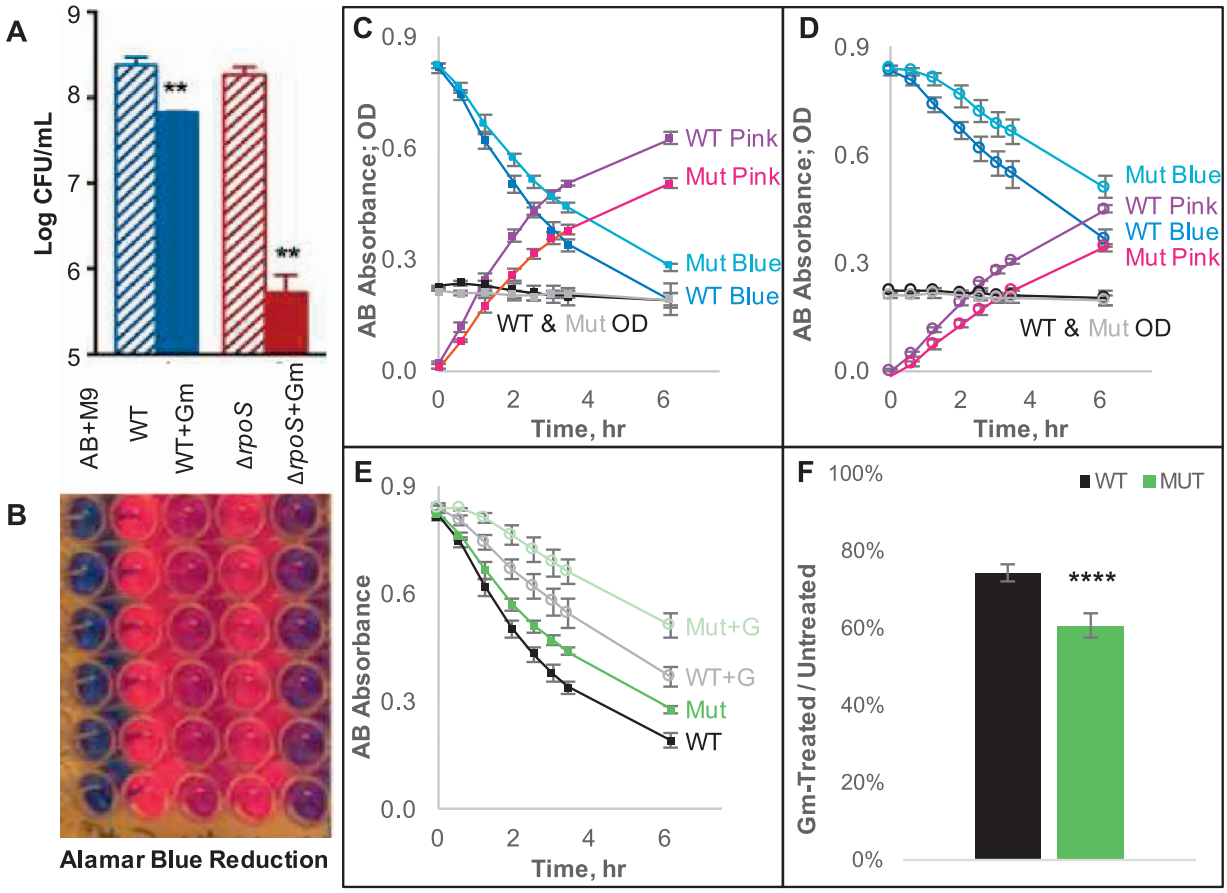

Fig. 3. (**A**) Counts of colony-forming units for wild type (WT) and Δ*rpoS* mutant strains of E. coli without and with gentamicin ("Gm") treatment at 16 μg/mL. (**B**) Color changes of Alamar Blue in 96-well plates due to metabolism of treated and untreated WT and Δ*rpoS* mutant; well-rows are aligned to corresponding bars of Panel A; control row ("AB + M9") shows initial, unchanged blue color of AB absent cellular metabolism. (**C**) Time dependence of relative concentrations of oxidized (blue/turquoise curves) and reduced (pink/magenta curves) forms of AB along with OD (turbidity; black/grey curves) due to wild type ("WT") and mutant ("Mut") cells in absence of Gm measured with a wellplate reader. (**D**) Same measurement as in Panel C but in the presence of 16 μg/mL Gm. (**E**) Time dependence of concentration of blue (oxidized) AB for each strain (WT in black/grey; mutant in green/light green) without and with Gm treatment. (**F**) Relative magnitude of the effect of Gm on the two strains based on the $t = 6$ h data from Panel E; each bar is normalized to the amount of AB reduction measured for the respective strain in absence of Gm treatment ($n = 6$; $p < 0.0001$). Error bars in Panels C through F are ± one standard deviation. (For interpretation of the references to colour in this figure legend, the reader is referred to the web version of this article.)

3.4. EcAMSat payload exerts additional stress, but can reproduce the rpoS-dependent UPEC resistance to Gm

We next determined if the AB method can assess Gm's effect on the two UPEC strains using the fluidic card delivery and optical systems of the *EcAMSat* platform. AB reduction was measured at the same wavelengths as for the plate experiments described above (Fig. 3). The payload is a closed environment and exposes UPEC to constituents, such as poly(methylmethacrylate), the acrylic-based pressure-sensitive adhesive, and poly(styrene) that can be stressful. Indeed, we found that cells in this setup grew more slowly: some 20 h were required for growth completion (Fig. 5B), as opposed to 6 h in conventional flasks (Materials and Methods). Given this relative sluggishness, we adjusted the times of stationary, Gm-treatment, and AB-viability phases of the experiments to 30, 45, and 50 h, respectively (see Fig. 5A).

The reduction of AB by wild type and mutant strains in the absence of Gm treatment is shown in Fig. 6A. There was a more marked difference in the metabolic activity of the untreated wild type and the mutant strains (Fig. 6A) in the payload setup than was seen in the plate experiments (Fig. 3C); this was unsurprising, given that the absence of the *rpoS* gene broadly weakens UPEC (Matin, 2014), and that the payload environment, as noted, is stressful. However, as in the plate experiment of Fig. 3, Gm retarded the dye reductive capability of the mutant to a higher extent (Fig. 6B). We normalized the reduction kinetics of AB by the two strains in the presence of Gm (Fig. 6D) by correcting for their respective untreated levels of activity. This was done, as in the experiment of Fig. 3, by dividing AB reduced in the presence of Gm by that reduced in its absence for all three concentrations of the drug.

In the well-plate experiment (Fig. 3), the untreated wild type had reduced 74% of the AB by the end of the experiment at 6 h. In the *EcAMSat* platform, for the experiment represented by Fig. 6, it took the untreated wild type 21 h to reduce an equivalent amount of dye. To permit comparison between the two setups, we have measured the normalized difference in the reductive capability of the wild type and the mutant strains at $t = 21$ h (see vertical red line, Fig. 6C), which is presented in the bar graph of Fig. 6D. This comparison reveals a significantly larger effect on the mutant relative to the wild type at all three doses of Gm, with the effect being most significant at the medium and high concentrations ($p = 0.00002$ and 0.0005, respectively), a result comparable to that obtained in the well-plate. This indicates that the physiological state determining the cellular response to Gm of the two strains remained similar in the two setups, strongly suggesting existence of comparable experimental conditions. Therefore, since biofilm formation did not occur in the microtiter plate experiments (see Materials and Methods), it is reasonable to posit its absence also in the *EcAMSat* platform. This is consistent with the fact that a post-experiment visual examination of the fluidic cards revealed no obvious indication of biofilm formation where they would be most readily observed, namely on the top and bottom cover films of the fluidic cards.

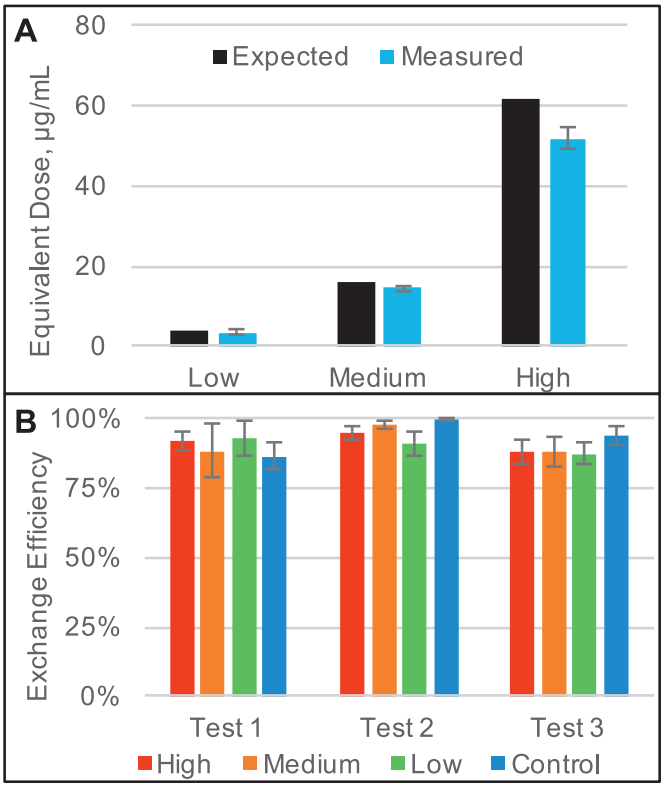

Fig. 4. (**A**) Expected (calculated) and optically measured (using dye) equivalent doses of Gm prepared using three separate "builds" of the EcAMSat fluidic system (different fluidic cards, tubing sets, pumps, and valves) for dye concentrations corresponding to low, medium, and high Gm levels; the "Measured" bars represent the averages of the results from the three builds. (**B**) Optically measured exchange efficiency of EcAMSat fluidic wells, shown individually for each of three separate builds of the fluidic system, after ~400 µL of exchange fluid were pumped through each 100 µL well by the fluidic system for the four banks of wells depicted in Fig. 1; all wells contained stationary-phase *E. coli* so as to include their impact on flow resistance through 0.2 µm pore-size filters at the inlet and outlet of each well (n = 12 wells per condition per test). Error bars in both panels are ± one standard deviation.

Given, however, that the flow of medium and other experimental reagents in this platform occurs towards the outlet microwell filters upon which some cells could be trapped and, further, that LSMMG and space MG enhance bacterial tendency to form biofilms (Lynch et al., 2006; McLean et al., 2001; Storrs-Mabilat, 2001), it is possible that a biofilm on (or in) the outlet filters could form in the ground tests and/or the planned space flight experiment. The potential effect of this possibility in space flight on the interpretation of the results is considered in the Discussion and Conclusions section. (In space microgravity, sedimentation being absent, biofilm formation preferentially at the bottom of the wells is highly unlikely and the same is likely true for the ground experiments due to the use of the "rotisserie" apparatus to prevent sedimentation (see Experimental section.)

We note that the comparison in Fig. 6D represents one of four nominally identical tests of the spaceflight experimental protocol. In all four of these tests, the high dose of Gm led to a (statistically meaningful) larger effect for the mutant than the wild type strain; for two of the four tests, the effect was also significant at the medium Gm concentration; the lowest Gm concentration produced a significant difference in just one of the four tests, the one shown in Fig. 6D. The reason the mutant exhibits differential sensitivity more reliably as drug concentration increases is not clear and will require further work to disentangle the interaction between the stresses of the payload system and that exerted by Gm. Nevertheless, it is clear that the system designed here is capable of answering the basic queries of interest, namely, would space MG increase Gm resistance of UPEC and would it do so in an *rpoS*-dependent manner?

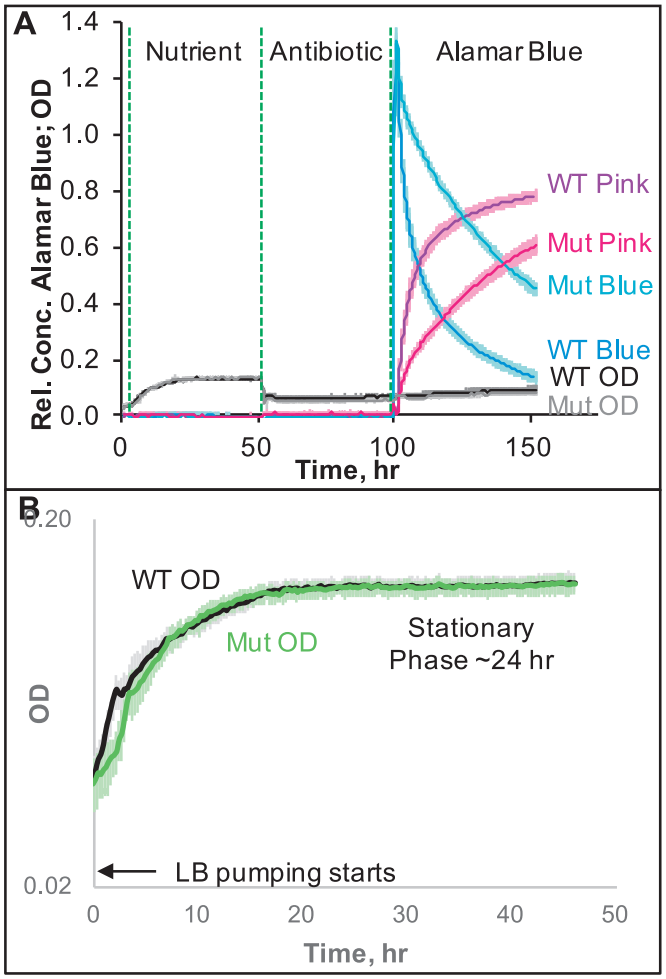

Fig. 5. (**A**) Time-dependent changes during growth, antibiotic-treatment, and Alamar-Blue-measurement phases of experiment using the EcAMSat optical system, fluidic card, and fluidic delivery system; results shown are for one of four nominally identical laboratory tests run according to the protocol to be used in the spaceflight experiment. Curves show absorbance of oxidized (blue/turquoise curves) and reduced (pink/magenta curves) forms of AB along with OD (turbidity; black/grey curves) due to wild type ("WT") and mutant ("Mut") cells. (**B**) Semi-log plot of OD due to cells (turbidity) from the growth phase of Panel A for wild type (black) and mutant (green) strains, showing the different growth phases. Error bars in both panels are ± one standard deviation. (For interpretation of the references to colour in this figure legend, the reader is referred to the web version of this article.)

3.5. Determination of bacterial viability and reagent strength with 'aging' during the stasis period

For our upcoming *EcAMSat* spaceflight experiment, there is some uncertainty concerning the interval of time that will elapse between the loading and integration of the payload constituents, including the bacteria in stasis, and the start of the experiment onboard the nanosatellite in a stable Earth orbit. Accordingly, we determined the effect of such a stasis period on bacterial viability and reagent strength; based on experience with *PharmaSat*, tests were conducted for a stasis period of 10 weeks. Consistent with previous studies (McCann et al., 1991), the Δ*rpoS* mutant retained less viability than the wild type: 0.3% vs. 0.7%. Gm was found to lose some 50% of its potency. AB and LB did not change their potency during this period. Also, viability of both strains over time in the dormant state was no worse in the payload hardware than in 96-well plates, indicating the hardware is biocompatible with the cells.

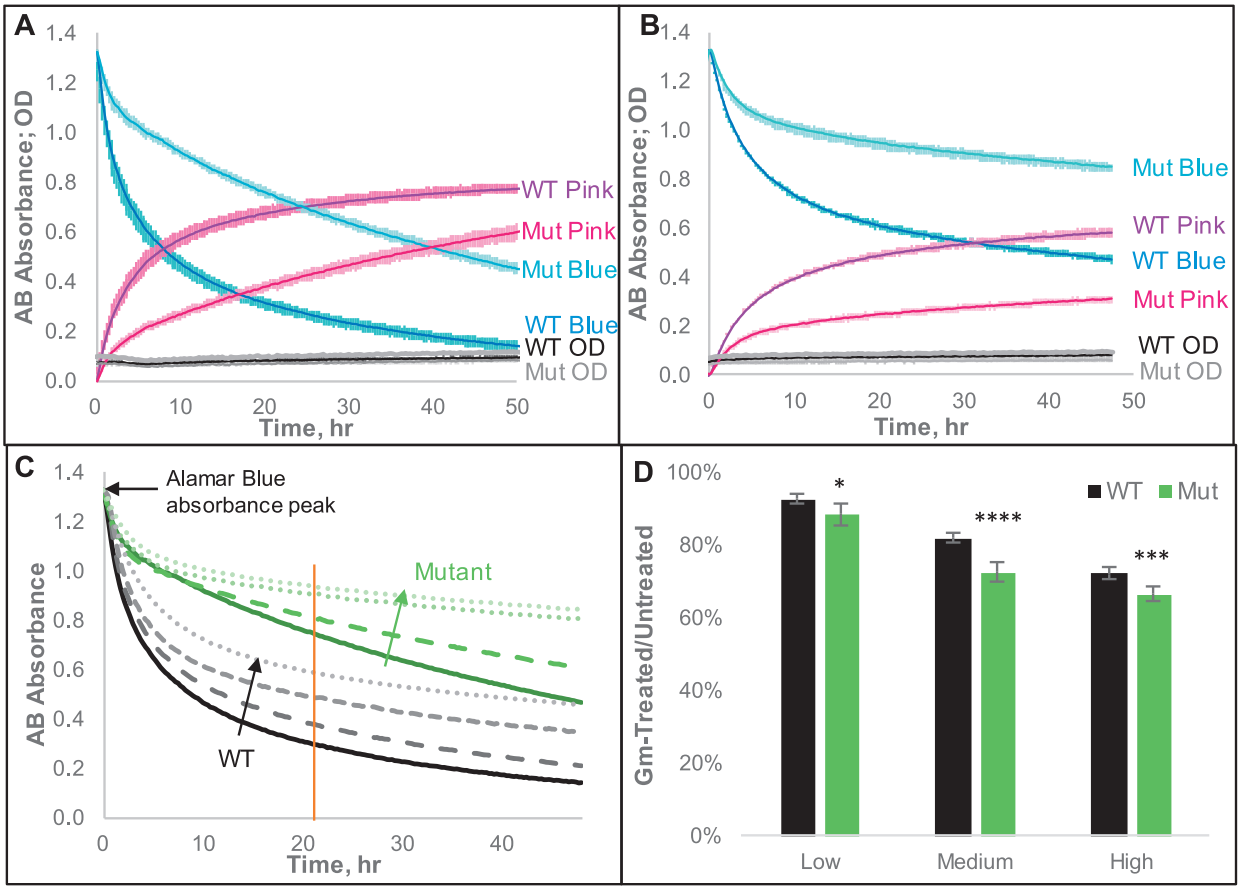

Fig. 6. (**A**) Time dependence of absorbance due to oxidized (blue/turquoise) and reduced (pink/magenta) forms of AB along with OD due to cells (turbidity; black/grey) for both E. coli strains in absence of Gm. (**B**) As in Panel A, but treated with Gm at 52 μg/mL. (**C**) Alamar Blue reduction curves (absorbance vs. time) for Gm = 0, 3.5, 14.6, and 52 μg/mL; diagonal arrows start at control (Gm = 0), point through low and medium doses, and terminate at highest dose. Vertical line at t = 21 h denotes point at which WT control has reduced 77% of Alamar Blue, equivalent to the t = 6 h data point of the conventional well-plate experiment shown in Fig. 3. (**D**) Amount of Alamar Blue reduced in presence of 3.5, 14.6, and 52 μg/mL Gm ("Low", "Medium", "High") normalized to the amount of AB reduced for the untreated control for each strain at t = 21 h of Panel C; p = 0.013 for the low dose, p = 0.00002 for the medium dose, and p = 0.005 for the high Gm dose. Error bars for Panels A, B, and D are ± one standard deviation. (For interpretation of the references to colour in this figure legend, the reader is referred to the web version of this article.)

4. Discussion and conclusions

The results show that the *EcAMSat* payload hardware, along with the experimental protocols we have developed and in combination with the advantages conferred by the use of a nanosatellite, are poised to provide an effective system to address the central query of this work: Does UPEC resistance to Gm increase in space MG and, if so, is it dependent on σ^s? Indeed, the *EcAMSat* approach offers a generic methodology for an in-depth study of bacterial drug resistance in space flight. σ^s is also required for a robust biofilm development, which represents a more resistant biological state; as stated above, LSMMG as well as space MG enhance *E. coli* tendency to form biofilms (Lynch et al., 2006; McLean et al., 2001; Storrs-Mabilat, 2001). Thus, biofilms may indeed form in the hardware during the space flight experiment with the Δ*rpoS* strain expected to form less abundant and less resistant biofilms than the wild type. This outcome, however, would not jeopardize the answering of our central query, because AB, besides being able to assess the viability of planktonic cells, is effective in assessing that of biofilms as well (Elkhatib and Noreddin, 2009). To the extent that biofilms with disparate resistances might be relevant to this study, it would be as regards *mechanistic aspects*; namely, how the loss of σ^s renders UPEC unable to raise its Gm resistance in space that we hypothesize will be found. We emphasize that we are attempting to determine *whether* σ^s has a role in any potential increase in Gm resistance in space MG; what might be the *mechanistic basis* of such a role, if it is found, is beyond the scope of this paper and could require follow-on space flight and/or ground experiments after data from *EcAMSat* have been telemetered and analyzed.

The possibility that bacterial drug resistance increases under microgravity is a major concern (Wilson et al., 2002; Bascove et al., 2009; Crucian et al., 2009; Mehta et al., 2000; Yi et al., 2016; Barrila et al., 2016; Wilson et al., 2007). Wilson et al. (2002, 2007) showed that, following culture on the Space Shuttle, *S. typhimurium* became more virulent in mice. Furthermore, the bulk of evidence from studies in LSMMG, which may approximate space MG, indicates that bacteria become broadly more resistant in MG to disinfectant agents (Gao et al., 2001; Lynch et al., 2004) and, as shown here, to an important antibiotic that is standard treatment for UTI, which has been reported in astronauts (Singh and Matin, 2016).

This potential danger of increased bacterial resistance is compounded by the fact that human immune response is compromised in space MG. After space flight, the oxidative burst capacity of monocytes and neutrophils of astronauts is diminished, as are the functions of their natural killer and T cells; cytokine production patterns are altered, likely accounting for the reactivation of herpesviruses seen in astronauts; stress hormones are increased; and there is a tendency to shift to the Th2 pattern (cytokine secretion resembling that of Th2 lymphocytes). Exposure to hypoxia or hyperoxia within the spacecraft or during spacewalks can further weaken the immune functions (Mehta et al., 2000; Yi et al., 2016; Gueguinou et al., 2009; Stowe et al., 2011a,b).

Bacterial antibiotic resistance has been previously examined in

space MG, but the results have been contradictory. While cultivation onboard Salyut 7 resulted in an increase in the minimum inhibitory concentration (MIC) of colistin and kanamycin acting on *E. coli* (Tixador et al., 1994), studies on the Space Station MIR indicated mostly decreased MICs for several antibiotics (Juergensmeyer et al., 1999). These pioneering studies, indicating the possibility of increased bacterial drug resistance in space, require further in-depth examination, a need addressed in this work; future work on this important subject will be greatly facilitated by the *EcAMSat* platform.

The dependence on σ^s of LSMMG-conferred heightened resistance of UPEC to Gm is akin to the role of this sigma factor in this resistance seen under Earth gravity, mentioned above (Wang et al., 2014). The latter studies identified several proteins of the antioxidant defense of this bacterium that can be targeted to enhance the efficacy of this drug. Examples span reactive-oxygen-species (ROS) quencher proteins (e.g., superoxide dismutase and catalase) and those of the pentose phosphate pathway that supply the NADPH that the quencher proteins require for their activity (e.g., glucose-6-phosphate, phosphogluconate dehydrogenases, and transaldolase A). We are at present screening small-compound libraries for inhibiting these proteins that could conceivably be used in synergy with Gm to enhance its efficacy. If the space flight experiment corroborates the LSMMG effect of σ^s-dependence of Gm resistance, such inhibitor compounds could prove valuable also in enhancing the effectiveness of Gm in treating infections in astronauts during space travel.

As regards *rpoS*, the hypothesis we aim to test in space flight is whether the absence of this gene renders UPEC unable to increase its Gm resistance in space MG as compared to the wild type. The answer, affirmative or negative, ends this aspect of the investigation. We suspect that the weakened antioxidant defense of the Δ*rpoS* mutant will play a role in this deficiency (if found), akin to that discovered in our conventional Earth studies (Wang et al., 2014). In addition, the potential diminished biofilm formation by the mutant will also likely contribute to the result. To what extent the diminished oxidative defense is responsible for this phenomenon would be a fit subject for future studies; it can be approached, for instance, by comparing Gm resistance in space flight of the Δ*rpoS* strain (defective in both antioxidant defense as well as biofilm formation) with a mutant missing any of the pairs of antioxidant defense proteins (Wang et al., 2014) (e.g., SodA/SodB) that impair Gm resistance in Earth gravity but do not interfere with biofilm formation. Given that the increase in bacterial resistance under LSMMG or space MG is controlled by the general stress response regulators, σ^s, it is reasonable to suspect that bacteria respond to MG as a deleterious stress comparable to other insults, like disinfectants and drugs mentioned above. The behavior of the Δ*rpoS* mutant in space flight experiments will critically test whether this is in fact the case by indicating whether any increase in resistance to Gm occurring in space MG is dependent on this gene.

There is apparent disagreement also with respect to other aspects of microbial biology between different studies in space flight studies. In several experiments on US Space Shuttle missions, Klaus et al. (1997) reported a shorter lag phase and a longer exponential phase in *E. coli* compared to ground controls, ascribing this effect to the formation of a 'pseudo-membrane' in the form of an osmotic solute gradient interfering with nutrient flux to the cells. Other studies, in contrast, have found that neither the lag nor the exponential phase in this bacterium is affected in space flight (Vukanti et al., 2012; Kacena et al., 1999). Our planned spaceflight experiments will shed light on these questions as well.

Contributions

The study was originally conceived by ACM and built upon as work progressed by NASA/Ames Research Center (ARC) colleagues. The applicability of AB for assessing the effect of Gm on UPEC viability was determined by J-HW and MK. The *EcAMSat* payload system, based on the previously flown *PharmaSat* spaceflight payload (Ricco et al., 2011; Parra et al., 2009), was adapted in order to execute the experiments reported here. Changes in system architecture and design were conceived by AJR, CCB, MPP, MC, and CRF. The biology experiment was adapted for compatibility with the *EcAMSat* payload hardware by MPP, MPL, and SC, who also conducted biology labwork at ARC with the participation of MRP and TNC. The fluidics system, with integrated optical measurement capability, was modified, developed, extensively tested and calibrated by MRP, TNC, MPL, MC, SSR, CMM, DTW, MXT, TDB, and CCB. Software and mechanical engineering work on the *EcAMSat* payload was accomplished by MC, CCB, AC, TVS, and CRF. AJR, MRP, and MPP developed and implemented data analysis methods. MBH managed NASA engineering configuration and documentation and SMS is the NASA *EcAMSat* project manager. ACM, MRP, MPP, and AJR wrote the manuscript.

Acknowledgments

This research was supported by NASA grant NNX10AM90A to A.M. at Stanford and by NASA's Space Life and Physical Sciences Research Division, Human Exploration and Operations Mission Directorate, at NASA/ARC.

References

Barrila, J., Wilson, J.W., Soni, A., Yang, J., Mark Ott, C., Nickerson, C.A., 2016. Using spaceflight and spaceflight analogue culture for novel mechanistic insight into *Salmonella* pathogenesis. In: Nickerson, A.C., Pellis, R.N., Ott, M.C. (Eds.), Effect of Spaceflight and Spaceflight Analogue Culture on Human and Microbial Cells: Novel Insights into Disease Mechanisms. Springer New York, New York, NY, pp. 209–235.

Bascove, M., Huin-Schohn, C., Gueguinou, N., Tschirhart, E., Frippiat, J.P., 2009. Spaceflight-associated changes in immunoglobulin VH gene expression in the amphibian Pleurodeles waltl. FASEB J. 23 (5), 1607–1615.

Cabeen, M.T., 2014. Stationary phase-specific virulence factor overproduction by a lasR mutant of Pseudomonas aeruginosa. PLoS One. 9 (2), e88743.

Crucian, B.E., Stowe, R.P., Mehta, S.K., Yetman, D.L., Leal, M.J., Quiriarte, H.D., et al., 2009. Immune status, latent viral reactivation, and stress during long-duration head-down bed rest. Aviat. Space Environ. Med. 80 (5 Suppl), A37–A44.

Dalebroux, Z.D., Svensson, S.L., Gaynor, E.C., Swanson, M.S., 2010. ppGpp conjures bacterial virulence. Microbiol. Mol. Biol. Rev. 74 (2), 171–199.

Elkhatib, W.F., Noreddin, A.M., 2009. A new fluorogenic assay for monitoring and determining planktonic and biofilm forms of Pseudomonas aeruginosa viable count in vitro. J. Rapid Meth. Aut. Mic. 17 (3), 304–314.

Gao, Q., Fang, A., Pierson, D.L., Mishra, S.K., Demain, A.L., 2001. Shear stress enhances microcin B17 production in a rotating w all bioreactor, but ethanol stress does not. Appl. Microbiol. Biotechnol. 56 (3-4), 384–387.

Gueguinou, N., Huin-Schohn, C., Bascove, M., Bueb, J.L., Tschirhart, E., Legrand-Frossi, C., et al., 2009. Could spaceflight-associated immune system weakening preclude the expansion of human presence beyond Earth's orbit? J. Leukoc. Biol. 86 (5), 1027–1038.

Hammond, T.G., Stodieck, L., Birdsall, H.H., Becker, J.L., Koenig, P., Hammond, J.S., et al., 2013. Effects of microgravity on the virulence of Listeria monocytogenes, Enterococcus faecalis, Candida albicans, and methicillin-resistant Staphylococcus aureus. Astrobiology. 13 (11), 1081–1090.

Hengge-Aronis, R., 2002a. Signal transduction and regulatory mechanisms involved in control of the sigma(S) (RpoS) subunit of RNA polymerase. Microbiol. Mol. Biol. Rev. 66 (3), 373–395 Table of contents.

Hengge-Aronis, R., 2002b. Stationary phase gene regulation: what makes an *Escherichia coli* promoter sigmaS-selective? Curr. Opin. Microbiol. 5 (6), 591–595.

Juergensmeyer, M.A., Juergensmeyer, E.A., Guikema, J.A., 1999. Long-term exposure to spaceflight conditions affects bacterial response to antibiotics. Microgravity Sci. Technol. 12 (1), 41–47.

Kacena, M.A., Merrell, G.A., Manfredi, B., Smith, E.E., Klaus, D.M., Todd, P., 1999. Bacterial growth in space flight: logistic growth curve parameters for *Escherichia coli* and *Bacillus subtilis*. Appl. Microbiol. Biotechnol. 51 (2), 229–234.

Kau, A.L., Hunstad, D.A., Hultgren, S.J., 2005a. Interaction of uropathogenic *Escherichia coli* with host uroepithelium. Curr. Opin. Microbiol. 8 (1), 54–59.

Kau, A.L., Martin, S.M., Lyon, W., Hayes, E., Caparon, M.G., Hultgren, S.J., 2005b. Enterococcus faecalis tropism for the kidneys in the urinary tract of C57BL/6 J mice. Infect. Immun. 73 (4), 2461–2468.

Klaus, D., Simske, S., Todd, P., Stodieck, L., 1997. Investigation of space flight effects on *Escherichia coli* and a proposed model of underlying physical mechanisms. Microbiology 143 (Pt 2), 449–455.

Kolter, R., Siegele, D.A., Tormo, A., 1993. The stationary phase of the bacterial life cycle. Annu. Rev. Microbiol. 47, 855–874.

Llorens, J.M.N., Tormo, A., Martinez-Garcia, E., 2010. Stationary phase in gram-negative bacteria. FEMS Microbiol. Rev. 34 (4), 476–495.

Lynch, S.V., Brodie, E.L., Matin, A., 2004. Role and regulation of sigma S in general

resistance conferred by low-shear simulated microgravity in *Escherichia coli*. J. Bacteriol. 186 (24), 8207–8212.
Lynch, S.V., Mukundakrishnan, K., Benoit, M.R., Ayyaswamy, P.S., Matin, A., 2006. *Escherichia coli* biofilms formed under low-shear modeled microgravity in a ground-based system. Appl. Environ. Microbiol. 72 (12), 7701–7710.
Mangan, M.W., Lucchini, S., Danino, V., Croinin, T.O., Hinton, J.C., Dorman, C.J., 2006. The integration host factor (IHF) integrates stationary-phase and virulence gene expression in *Salmonella enterica serovar Typhimurium*. Mol. Microbiol. 59 (6), 1831–1847.
Matin, A., 1991. The molecular basis of carbon-starvation-induced general resistance in *Escherichia coli*. Mol. Microbiol. 5 (1), 3–10.
Editor-in-Chief A. Matin, A.2009. Stress, bacterial: general and specific. In: Moselio, S. (Ed.), Encyclopedia of Microbiology, third ed. Academic Press, Oxford, pp. 485–500.
Matin, A., Auger, E.A., Blum, P.H., Schultz, J.E., 1989. Genetic basis of starvation survival in nondifferentiating bacteria. Annu. Rev. Microbiol. 43, 293–316.
Matin, A.C., 2014. Stress, Bacterial: General and Specific☆. Reference Module in Biomedical Sciences. Elsevier.
McCann, M.P., Kidwell, J.P., Matin, A., 1991. The putative sigma factor KatF has a central role in development of starvation-mediated general resistance in *Escherichia coli*. J. Bacteriol. 173 (13), 4188–4194.
McLean, R.J., Cassanto, J.M., Barnes, M.B., Koo, J.H., 2001. Bacterial biofilm formation under microgravity conditions. FEMS Microbiol. Lett. 195 (2), 115–119.
Mehta, S.K., Pierson, D.L., Cooley, H., Dubow, R., Lugg, D., 2000. Epstein-Barr virus reactivation associated with diminished cell-mediated immunity in antarctic expeditioners. J. Med. Virol. 61 (2), 235–240.
Mouslim, C., Hughes, K.T., 2014. The effect of cell growth phase on the regulatory cross-talk between flagellar and Spi1 virulence gene expression. PLoS Pathog. 10 (3), e1003987.
Nicholson, W.L., Ricco, A.J., Agasid, E., Beasley, C., Diaz-Aguado, M., Ehrenfreund, P., et al., 2011. The O/OREOS mission: first science data from the Space Environment Survivability of Living Organisms (SESLO) payload. Astrobiology 11 (10), 951–958.
Parra, M., Ly, D., Ricco, A., McGinnis, M., Niesel, D., 2009. The PharmaSat Nanosatellite platform for life science experimentation: effects of spaceflight on antifungal activity against *Saccharomyces cerevisiae*. Gravitational Space Biol. 23 (30), 30.
Rampersad, S.N., 2012. Multiple applications of Alamar Blue as an indicator of metabolic function and cellular health in cell viability bioassays. Sensors (Basel) 12 (9), 12347–12360.
Ricco, A.J., Parra, M., Niesel, D., Piccini, M., Ly, D., McGinnis, M., et al., 2011. PharmaSat: drug dose response in microgravity from a free-flying integrated biofluidic/optical culture-and-analysis satellite. In: Proc SPIE. 79290T.
Roop 2nd, R.M., Gee, J.M., Robertson, G.T., Richardson, J.M., Ng, W.L., Winkler, M.E., 2003. Brucella stationary-phase gene expression and virulence. Annu. Rev. Microbiol. 57, 57–76.
Singh, R., Matin, A.C., 2016. Cellular response of *Escherichia coli* to microgravity and microgravity analogue culture. In: Nickerson, A.C., Pellis, R.N., Ott, M.C. (Eds.), Effect of Spaceflight and Spaceflight Analogue Culture on Human and Microbial Cells: Novel Insights Into Disease Mechanisms. Springer New York, New York, NY, pp. 259–282.
Sonenshein, A.L., 2005. CodY, a global regulator of stationary phase and virulence in Gram-positive bacteria. Curr. Opin. Microbiol. 8 (2), 203–207.
Storrs-Mabilat, M., 2001. Study of a Microbial Detection System for Space Applications. Second Workshop on Advanced Life Support, Noordwijk, The Netherlands.
Stowe, R.P., Kozlova, E.V., Sams, C.F., Pierson, D.L., Walling, D.M., 2011a. Latent and lytic Epstein-Barr virus gene expression in the peripheral blood of astronauts. J. Med. Virol. 83 (6), 1071–1077.
Stowe, R.P., Sams, C.F., Pierson, D.L., 2011b. Adrenocortical and immune responses following short- and long-duration spaceflight. Aviat. Space Environ. Med. 82 (6), 627–634.
Tixador, R., Gasset, G., Eche, B., Moatti, N., Lapchine, L., Woldringh, C., et al., 1994. Behavior of bacteria and antibiotics under space conditions. Aviat. Space Environ. Med. 65 (6), 551–556.
Vukanti, R., Model, M.A., Leff, L.G., 2012. Effect of modeled reduced gravity conditions on bacterial morphology and physiology. BMC Microbiol. 12, 4.
Wang, J.H., Singh, R., Benoit, M., Keyhan, M., Sylvester, M., Hsieh, M., et al., 2014. Sigma S-dependent antioxidant defense protects stationary-phase *Escherichia coli* against the bactericidal antibiotic gentamicin. Antimicrob. Agents Chemother. 58 (10), 5964–5975.
Wilson, J.W., Ott, C.M., Honer zu Bentrup, K., Ramamurthy, R., Quick, L., Porwollik, S., et al., 2007. Space flight alters bacterial gene expression and virulence and reveals a role for global regulator Hfq. Proc. Natl. Acad. Sci. U S A. 104 (41), 16299–16304.
Wilson, J.W., Ott, C.M., Ramamurthy, R., Porwollik, S., McClelland, M., Pierson, D.L., et al., 2002. Low-Shear modeled microgravity alters the *Salmonella enterica* serovar typhimurium stress response in an RpoS-independent manner. Appl. Environ. Microbiol. 68 (11), 5408–5416.
Woellert, K., Ehrenfreund, P., Ricco, A.J., Hertzfeld, H., 2011. Cubesats: Cost-effective science and technology platforms for emerging and developing nations. Adv. Space Res. 47 (4), 663–684.
Yi, B., Crucian, B., Tauber, S., Ullrich, O., Choukèr, A., 2016. Immune Dysfunction in Spaceflight: An Integrative View. In: Nickerson, A.C., Pellis, R.N., Ott, M.C. (Eds.), Effect of Spaceflight and Spaceflight Analogue Culture on Human and Microbial Cells: Novel Insights Into Disease Mechanisms. Springer New York, New York, NY, pp. 61–79.
Zgurskaya, H.I., Keyhan, M., Matin, A., 1997. The sigma S level in starving *Escherichia coli* cells increases solely as a result of its increased stability, despite decreased synthesis. Mol. Microbiol. 24 (3), 643–651.